AIAA-2002-0258
Optimum Spanloads in Formation Flight

S. Iglesias and W.H. Mason
Virginia Polytechnic Institute and State University
Blacksburg, VA

40th AIAA Aerospace Sciences Meeting & Exhibit
14-17 January 2002 / Reno, NV

Optimum Spanloads in Formation Flight

Sergio Iglesias[*] and William H. Mason[†]
Department of Aerospace and Ocean Engineering
Virginia Polytechnic Institute and State University
Blacksburg, VA 24061-0203

Formation flight can result in large induced drag reductions. Optimum spanloads for a group of aircraft flying in an arrow formation were found using a discrete vortex method with a Trefftz plane analysis under constraints in lift, pitching moment and rolling moment coefficients. It has been shown that large reductions in induced drag can be obtained when the spanwise and vertical distances between aircraft are small. In certain cases this results in negative induced drag (thrust) on some airplanes in the configuration. The optimum load distributions necessary to achieve these benefits may, however, correspond to a geometry that will produce impractical lift distributions if the aircraft are flying alone. Optimum separation among airplanes in this type of formation is determined by such diverse factors as the ability to generate the required optimum load distributions or the need for collision avoidance.

I. Introduction

A group of aircraft flying in formation will experience induced drag savings due to the upwash coming from nearby airplanes. Formation flight benefits can be observed in nature in the flying disposition of migrating birds, often adopting V-shaped configurations. These formations help birds save energy by decreasing drag so that they can travel longer distances.

The variability in geometry of bird's wings, together with their highly controllable flight, allows them to change their wing geometry and fly very close to each other. This allows them to take full advantage of formation flying. For a rigid wing aircraft the capability of adapting wing geometry is very limited. Close flying is difficult because of collision dangers and, until recently, precision control problems. In this paper the advantages of formation flying will be studied as a function of relative distance between aircraft, and the adaptability and limitations of rigid aircraft will impose restrictions on the benefits that can actually be achieved.

Formation flight has been studied frequently in the past. For example, Schollenberger and Lissaman[1] investigated the formation flight of birds. They realized that the bird flexibility was an important requirement to obtain maximum advantage in formation flying. Their analysis showed that a 40% induced drag reduction could be achieved for each bird flying in an arrow formation consisting of just three birds. According to these authors, when 25 birds were flying in an arrow formation, induced drag savings as large as 65% could be achieved for each bird, and this drag reduction could result in a range increase of about 71%. Feifel[2] used a vortex lattice method with calculations performed in the near field to compute the advantages of formation flying in an array of five airplanes of specified geometry flying in a V-formation. Feifel only shows results for one test case, so that the magnitude of the induced drag reduction and its variation with spacing between aircraft was not shown. Maskew[3], also using a vortex lattice method, but with a Trefftz plane analysis, studied the induced drag variation for each aircraft and for the whole formation as a function of the distance (in the three space coordinates) between airplanes for an arrow formation consisting of three equal aircraft.

In the last decade formation flying has again become of interest.[4] Beukenberg and Hummel[5] studied formation flying, presenting flight test data for three aircraft flying in an arrow formation, and comparing the data to theoretical

[*] Graduate Student, Department of Aerospace and Ocean Engineering, Student Member AIAA, now at Gamsea, Spain
[†] Professor, Department of Aerospace and Ocean Engineering, Associate Fellow AIAA, mason@aoe.vt.edu

aerodynamic results obtained with various vortex models. Blake and Multhopp[6] also examined the problem recently. This was followed by experimental investigations performed by Gingras[7] who did wind tunnel experiments to investigate the aerodynamic effects of a lead aircraft on a trail aircraft in close formation.

When dealing with arrow formations, all the aircraft that are off-center will have an asymmetrical load distribution due to the upwash distribution coming from the other airplanes. Of course the rolling moment coefficient must be zero for each aircraft in the formation. In their studies, Feifel[2] and Maskew[3] used aircraft of completely known geometry, that is, the twist distribution was specified for the wings (no twist for both authors) and aileron deflection was used to set rolling moment coefficient zero.

A different approach was followed here, where no twist or camber distribution is known before-hand, and the loads are calculated to obtain minimum induced drag for the whole formation under individual aircraft constraints of lift coefficient and rolling moment coefficient. While Feifel and Maskew solved an analysis problem with known geometry, this paper addresses a design problem for which the twist and camber distribution is not known. Instead, the actual geometry must be found after the calculations are made to find the required load distributions. Attacking the problem in a design mode will give maximum achievable benefits for the whole formation.

II. General Approach

Airplanes in formation flight can obtain large advantages in induced drag reductions as a result of the influence that the upwash from other aircraft exert on them. A code has been developed to obtain the optimum spanload distributions for a group of airplanes flying in a V-formation. Only aerodynamic considerations are taken into account, with no structural constraints.

The main purpose of the code developed is to find the optimum spanload that gives minimum induced drag for the whole system of airplanes. The induced drag for each aircraft alone will also be of primary importance to study the effects of relative position on individual aircraft performance. Induced drag will be the measure of effectiveness, both for the formation and for the single aircraft.

An important aspect of the code developed and the studies performed must be pointed out. The flow is being modeled as potential, inviscid flow. A potential flow vortex model representation is being used. These models usually give quite good results for regions that are not near the vortex cores, which are small, where viscous effects become important.

A description of the aerodynamics code used for optimum load distribution design and induced drag calculations follows.

III. Description of the Aerodynamics Code

A code written by Grasmeyer[8] (*idrag* version 1.1), which applies the theories developed by Blackwell[9], Lamar[10], Kuhlman[11] and Kroo[12] was modified here. This theory is a discrete vortex method with a Trefftz plane analysis to calculate spanloads corresponding to the minimum induced drag of the configuration.

The code also includes an optional trim constraint, in which the pitching moment coefficient can be fixed if several surfaces are analyzed. Given the geometry for a number of surfaces, the program finds the spanload that gives minimum induced drag for a specific value of lift coefficient and moment coefficient using the method of Lagrange multipliers[8].

Several modifications have been made to this code to include the capability of analyzing several aircraft configurations. First, a lift coefficient constraint is now necessary for each aircraft. A trim constraint on the rolling moment and the pitching moment of individual aircraft in the formation is also required.

The code now assumes that the configuration is always symmetric, so that the geometry of V-formations can be specified only with the central aircraft and one side of the formation. The central aircraft, due to symmetry, will have an equal load distribution on both sides. Off-center airplanes, on the contrary, will have asymmetrical spanloads because the formation does not meet the symmetry condition from their point of view. This asymmetry causes these airplanes to have non-zero rolling moment coefficients about their centers of gravity, so that an extra constraint to maintain rolling moment coefficient for off-centered aircraft equal to zero has also been imposed.

Optimum load distributions for a group of airplanes flying in the V-formation is found using the method of Lagrange Multipliers under the constraints of a specified lift coefficient for each aircraft, a pitch trim constraint for each, and a rolling moment coefficient constraint for all except the central one.

Another major modification has been introduced in the code to allow the analysis and induced drag calculations of separate airplanes.

The code used (*idrag* version 1.1) is merely an implementation of the equations used by Blackwell[9]. This theory makes use of Munk's Stagger Theorem[13]. According to the theorem, the induced drag of the entire system is independent of the streamwise location of the spanloads. Once the optimum load distribution for the whole configuration has been found, that will always be the optimum no matter what changes in the streamwise location of different aircraft in the formation are made, and the formation induced drag will always remain the same. For this reason, Blackwell's theory makes the induced drag calculations in the Trefftz plane. The Trefftz plane is located at an infinite distance downstream of the lifting surfaces. Making the calculations in this plane allows Blackwell to ignore streamwise effects.

For a formation configuration, where the interest lies not only in the induced drag as a whole, but rather on the induced drag of each airplane, Blackwell's theory is not completely applicable. This is because the induced drag of each lifting surface *is* dependent on its streamwise position although the total induced drag of all the aircraft is not.

The code was modified by assigning a streamwise coordinate position to each discrete vortex. The downwash angles are calculated on the lifting surfaces at the midpoint of each discrete bound vortex line. Calculations are now performed in the near field, and not in the Trefftz plane. The influence of each trailing vortex on each force point was modified applying Biot-Savart law in the streamwise direction and the influences of the bound vortex lines on the force points were also added. In that way, optimum spanloads are still independent of streamwise vortex locations, but individual downwash angles and induced drags have a strong dependence on movements along this axis (total induced drag of the complete system remains unchanged). To obtain accurate nearfield induced drag calculations using this approach the bound vortices must not be swept. This requirement was proven theoretically by Jan Tulinius[14], and was proven numerically in this work.

Forces are calculated at the midpoint of the bound vortex lines to obtain a quick and simple way for finding minimum drag spanloads, while performing the calculations in the near field. Loads at each station are assumed to be applied at the same location. If the induced angle is known here, the induced drag at each station is simply the induced angle times the corresponding load. However, there is one slight complication. The relation between the loads at each station and the wing geometry (twist or camber) at that station has not been established. Thus at this point we have not found the twist or camber distribution required to obtain the spanload.

With the code modified, results can be obtained that give total and individual drag savings as a function of aircraft relative distances to each other. The optimum load distributions required to achieve these drag benefits are also obtained. Complete details, including the mathematical derivations, are given in the thesis by Iglesias[15], which is available electronically.

IV. Results for equal aircraft

Optimum load distributions for a group of three equal aircraft flying in an arrow formation will be found, and their induced drag compared as a function of relative distance in the three space directions. Planform geometry and the relative spacing between aircraft are the same as in Maskew's[3], with three airplanes, each one of them consisting only of planar wing panels so that pitching moment constraints do not need to be applied. Each planform is trimmed with respect to rolling moment. The characteristics of the planform geometry are given in **Table 1** (from Maskew[3]).

Table 1. Basic wing geometry

Span	**2.0**
Geometric mean chord	**0.25**
Area	**0.5**
Aspect ratio	**8.0**
Taper ratio	**0.33**
Sweepback (quarter-chord line)	**5 deg**
Dihedral	**0**

The aircraft will be moved relative to each other in the *x* (streamwise), *y* (spanwise) and *z* (vertical) directions, studying the effects of these distances on load distributions and drag savings. **Figure 1** shows how the off-center airplane will be moved relative to the central one. Recall that it is assumed that the configuration will always be symmetric.

The off-center aircraft (*Aircraft 2*) will be moved along the heavy bold line in **Figure 1**. First, from x/b = -3.0 to x/b = +3.0, the variation in induced drag savings will be studied as a function of streamwise distance, maintaining *y/b*=0.89 and *z/b*=0.01. This small, but still significant value of vertical offset between airplanes is used due to numerical problems in the code when the projections of different lifting surfaces in the Trefftz plane lay on top of each other.

Then, with a fixed *x/b* = 3.0, the spanwise effect will be considered by letting *z/b* = 0.01 and changing *y/b*. Finally, the vertical effect is obtained by letting *z/b* vary while setting *x/b* = 3.0 and *y/b* = 0.89. This is similar to the approach used by Maskew[3].

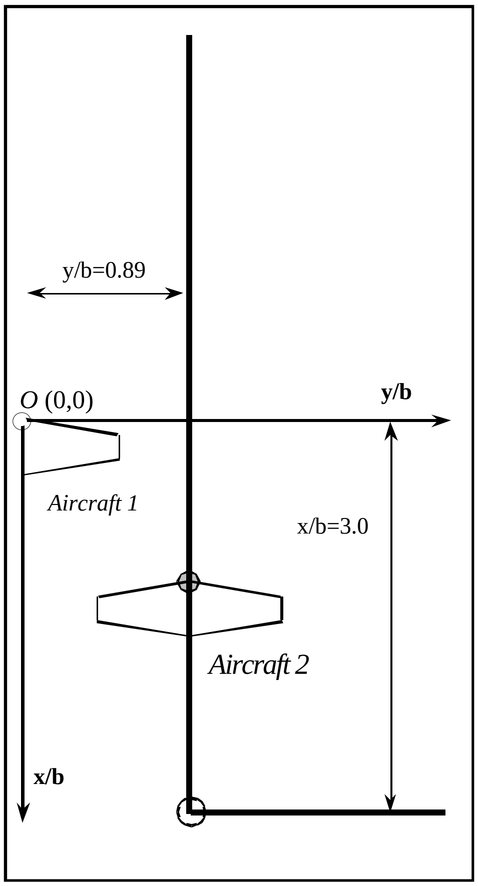

Figure 1. Movement of the off-centered aircraft relative to the central one (from Maskew[3])

Although the planform geometry and movements of the airplanes are taken from Maskew's paper, the main purpose here is not to compare results. The geometric similarities will certainly make them resemble his results. However, Maskew solves an analysis problem in which the wing twist distribution is specified and the aileron deflection is found so that rolling moment equals zero. With the whole wing geometry fixed, downwash angles completely determine the loads at each station.

In this paper a design problem is treated, in which only planform geometry is known and optimum loads are found. This time the loads are not determined by the downwash angles satisfying a surface boundary condition. Instead, we determine the loads and downwash angles from the requirement of minimum induced drag for the formation, together with the imposed constraints on lift and rolling moment.

To set the rolling moment coefficient to zero in the design problem, the aileron used by Maskew will not be useful, because calculations are not dependent on twist or camber, and therefore, angle of attack. In a sense, the entire wing is considered to be a control surface and the rolling moment constraint is applied to each wing through a constraint on the spanload.

A. Streamwise Effect

Airplane 2 is moved along the *x*-axis from *x/b*=-3 to *x/b*=3 as shown in **Figure 1**. **Figure 2** shows the change in induced drag coefficient for each aircraft and for the formation as the streamwise relative distance is changed. Results are shown as the ratio of their induced drag in the formation to their induced drag when flying alone. Induced drag for single flight is the minimum induced drag for an aircraft alone configuration, corresponding to an elliptic lift distribution and a span efficiency factor equal to 1.

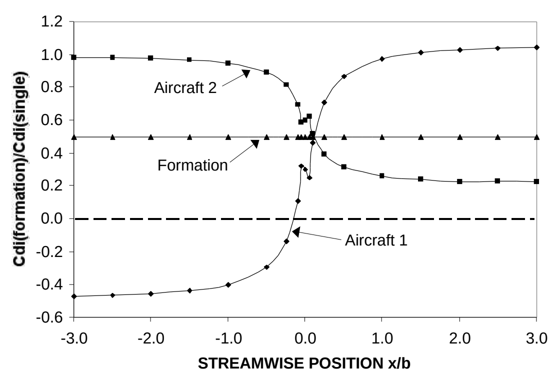

Figure 2. Effect of streamwise position, *y/b*=0.89, *z/b*=0.01.

Note that the induced drag for the formation is independent of the streamwise location of the airplanes, as stated by Munk's theorem. That constant value is the minimum induced drag for the whole configuration. The optimum spanloads corresponding to this minimum drag are shown in **Figure 3** (only shown half). The load distribution is also independent of streamwise position, so that **Figure 3** shows the spanload for any *x/b*.

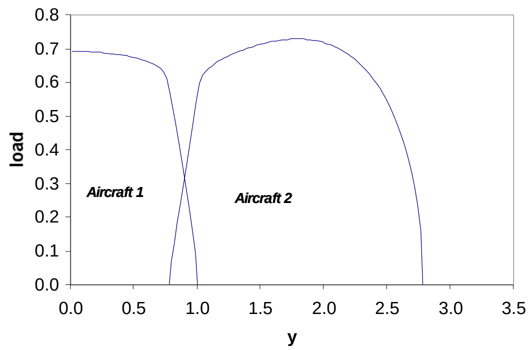

Figure 3. Optimum load distribution *z/b*=0.01, *y/b*=0.89

The induced drag coefficients of *Aircraft 1* and *Aircraft 2* are highly dependent on *x* when the aircraft are close in this direction. For a streamwise distance between them greater than three spans, their induced drag reaches a steady value and is no longer dependent on *x* separation.

When *x/b* is negative, the central aircraft is behind the two leading ones, so that it receives the upwash from them. The result is that *Aircraft 1* has a negative induced drag (a thrust forward). The upwash from the leading aircraft is higher than the downwash caused by the central aircraft on itself.

For *x/b* positive, the central aircraft is leading the formation, and its upwash influences *Aircraft 2* reducing its induced drag. This time, since it is only the central aircraft influencing two trailing ones, the upwash contribution by *Aircraft 1* on *Aircraft 2* is lower than the downwash caused by *Aircraft 2* on itself.

When *Aircraft 1* leads the formation with a high streamwise separation with respect to *Aircraft 2* (see **Figure 2** for *x/b*=3), its induced drag ratio is greater than one. The induced drag coefficient when flying alone was established to be the minimum induced drag, corresponding to an elliptical load distribution. Then, the leading aircraft suffers a decrease in performance. This seems contradictory, since almost no downwash should be felt on *Aircraft 1* due to *Aircraft 2* (it is far aft). However, this increase in induced drag coefficient enhances the performance of the trailing airplanes, so that a formation minimum induced drag is obtained. **Figure 3** shows that the load distribution for the central aircraft is not elliptic. It has higher loads toward the wing tip than an elliptically loaded wing would have. These high loads towards the tip induce greater upwash angles on the trailing aircraft, reducing their induced drag coefficients. The result is that a decrease in performance in the leading aircraft can help obtaining overall drag reductions for the formation.

The same thing happens for a high negative value of *x/b*. In this case the off-center airplanes lead the formation and they experience a reduction in performance due to their non-elliptic load distributions. Here, however, the two leading aircraft influence each other so that their induced drag increase is compensated by the upwash they exert on each other.

For *x/b* near zero, the induced drag curves for *Aircraft 1* and *Aircraft 2* have a break (see **Figure 2**). This is caused by the influence of the bound vortex lines on the airplanes. If *Aircraft 1* leads the formation, it feels an upwash from the bound vortex lines of the trailing aircraft, and exerts a downwash on them. When they cross, the upwash and downwash influences are inverted and a break in the induced drag curve appears. The break is a lot smoother if vertical or spanwise distance is increased (for a *y/b* = 0.94 the break no longer appears). Note that a streamwise distance near zero with a vertical distance as small as 0.01 is not really a physically achievable situation.

One further consideration must be pointed out. **Figure 3** shows the asymmetry in the load distribution of *Aircraft 2*. This asymmetry is a consequence of a V-formation geometry, in which only the central aircraft has a symmetric lift distribution. Despite the asymmetric spanload on *Aircraft 2*, its rolling moment coefficient about its center of gravity is zero (the rolling moment constraint was active). Achieving the desired lift distribution will be the greatest problem, not only because of the asymmetry of the load distribution, but because the spanloads will be dependent on vertical and spanwise distance between airplanes.

B. Spanwise Effect

Aircraft 2 is moved along the *y* direction while *x/b* is fixed at a value of 3.0 and *z/b*=0.01. **Figure 4** shows the changes in induced drag for each aircraft and the whole formation as the spanwise distance is varied.

The formation induced drag coefficient is highly dependent on spanwise separation. When *y/b*=1 the right tip of *Aircraft 1* coincides with the left tip of *Aircraft 2* in *y* location. The formation minimum actually occurs for a value of *y/b* less than one, where *Aircraft 2* is in the wake of the leading aircraft. For a spanwise distance of two spans, the drag savings are very small and formation flying is no longer beneficial. Thus, it is important to maintain the airplanes in close spanwise position to obtain any significant induced drag reduction.

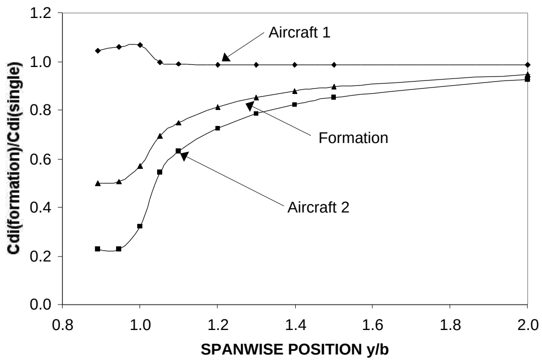

Figure 4. Effect of spanwise position, *x/b*=3.0, *z/b*=0.01.

The drag dependence of *Aircraft 2* on spanwise distance is also very strong, with 80% potential induced drag savings for optimum position. *Aircraft 1*, however, has a constant induced drag coefficient equal to its minimum induced drag when flying alone as long as the airplane tips do not get close in the spanwise direction. If the aircraft tips come close or overlap, *Aircraft 1* performance decreases, while the induced drag for *Aircraft 2* and the formation starts decreasing more rapidly.

The previous section showed how a decrease in performance in *Aircraft 1* could produce an induced drag decrease for the trailing airplanes, and in turn for the whole formation. But it is necessary to see why this effect only takes place for close spanwise distances. **Figure 5** shows the optimum load distributions for several spanwise positions.

When the airplane tips start overlapping, their optimum load distributions are very different from the elliptical loading, the main difference being higher loads in the vicinity of the other aircraft's tip. These loads increase drag on *Aircraft 1* but induce a greater upwash on *Aircraft 2*, improving its performance. That is why **Figure 4** shows a rise in induced drag when tips overlap.

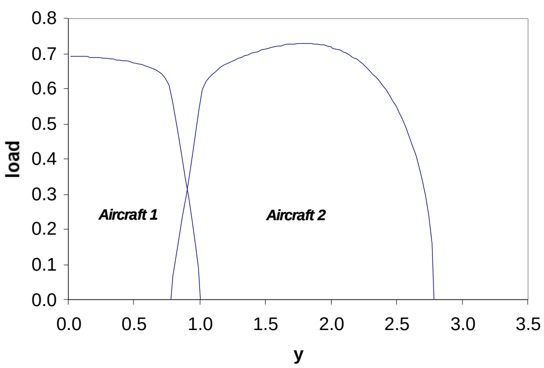

a) *z/b* = 0.01, *y/b* = 0.89

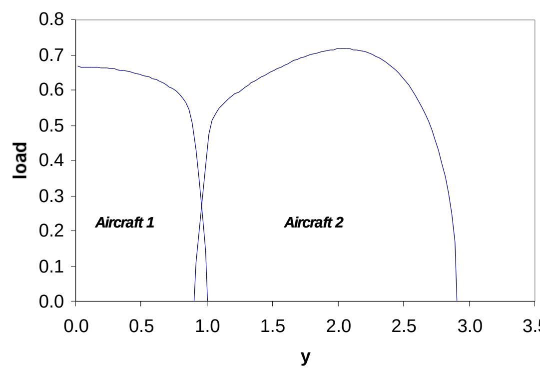

b) *z/b* = 0.01, *y/b* = 0.95

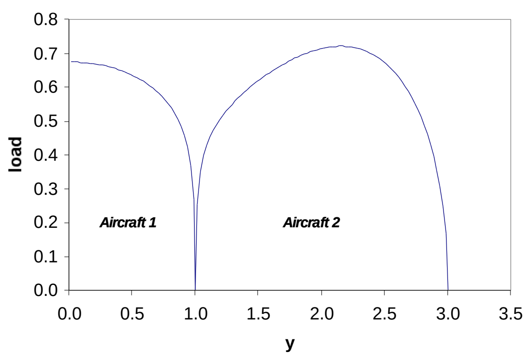

c) *z/b* = 0.01, *y/b* = 1.00

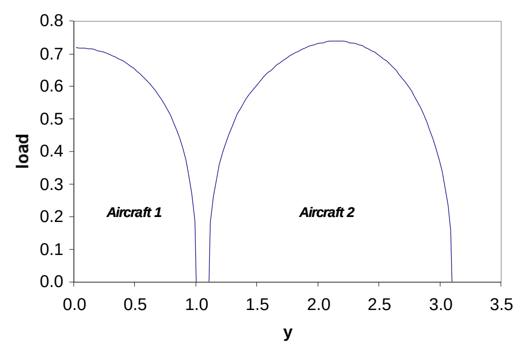

d) *z/b* = 0.01, *y/b* = 1.05

Figure 5. Optimum load distribution for different spanwise distances

For a tip spanwise distance greater than *y/b*=1, the overlapping does not occur, and the optimum load distributions for both airplanes become nearly elliptic. Their spanloads are now close to the optimum for single flight. In this situation, higher loads towards the aircraft tip will again decrease leading aircraft performance helping the trailing airplanes. However, the induced upwash on *Aircraft 2* will be much smaller when the aircraft do not overlap (note that induced velocities are inversely proportional to spanwise distance). The result is that the reduction in the trailing aircraft drag will not compensate for the drag increase on the leading aircraft. The formation minimum corresponds to load distributions close to those for solo flight when aircraft tips do not overlap.

The fact that a potential flow vortex model is used in this analysis should be emphasized here. Overlapping tips means close vortex interactions, where potential flow can fail and viscous effects may need to be included.

C. Vertical Effect

Aircraft 2 is moved in the vertical direction while keeping *y/b*=0.89 and *x/b*=3.0. The induced drag variation is shown in **Figure 6**.

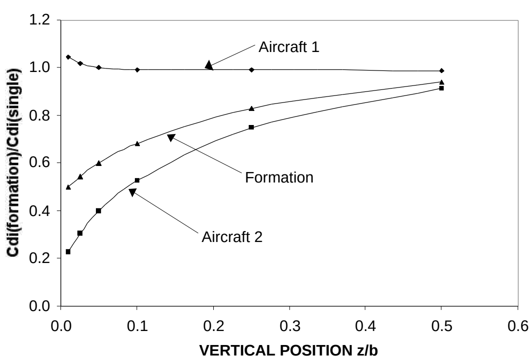

Figure 6. Vertical effect, *x/b*=3.0, *y/b*=0.89.

The strong dependence on *z* location is clear from this figure. Maximum drag reductions for the formation occur at *z*=0 (induced drag variation will be equal for negative values of vertical position). The actual drag reduction values at *z*=0 are not obtained due to numerical problems at these very close vertical locations.

When the vertical distance between aircraft is small (less than 0.05), optimum load distributions start deviating from their elliptical shapes, having higher loads near the tip. A decrease in *Aircraft 1* performance that helps formation drag is again observed. The load distribution change with vertical position is similar to that obtained with spanwise distance variation (**Figure 5**).

V. Results for different aircraft sizes

Recently, interest has been concentrated on systems of airplanes consisting of a leading, large size mother aircraft and two smaller aircraft on its side, trailing the formation. The greater loads that the mother aircraft experiences in flight produce large upwash velocities that can be used by the trailing airplanes. In this way smaller, less efficient airplanes can get large drag benefits from big, efficient aircraft with long ranges.

The configuration studied here is shown in **Figure 7**. The planform characteristics of the mother aircraft are given in **Table 2**. *Aircraft 2* geometry is exactly equal to that of the leading aircraft, with a scale factor of 0.5. That is, *Aircraft 1* is exactly twice as large as *Aircraft 2*. The lift coefficients of both airplanes are set to a value of 0.6.

Note that the airplanes now have tail panels, so that the pitching moment coefficient can be included in the calculations. Optimum spanloads for minimum induced drag are found with constraints in lift, pitching moment and rolling moment coefficients.

Since the smaller, off-center aircraft are the ones that must receive drag benefits from the central one; they are located trailing the formation. The streamwise distance between aircraft is set to be large enough so that aircraft collision can be avoided and induced drag coefficients are independent of *x* direction. **Figure 2** showed that *Aircraft 2* obtains the largest benefit at this position. **Figure 6** also shows that vertical spacing between aircraft must approach zero for maximum drag reductions. So, in this study *x/b* will be set to 3.0 and *z/b*=0.01. These values are non-dimensionalized by the span of the mother aircraft (*b*=1.0). The small vertical spacing again avoids numerical problems.

Only the spanwise effect will be studied this time, since it will give maximum induced drag reductions for the trailing airplanes. The induced drag variation for each aircraft and the formation as a function of relative spanwise distance is shown in **Figure 8**. Spanwise position is non-dimensionalized by the span of *Aircraft 1*. As in the previous case, when *y/b*=1 the tips of the different aircraft are in the same *y* position.

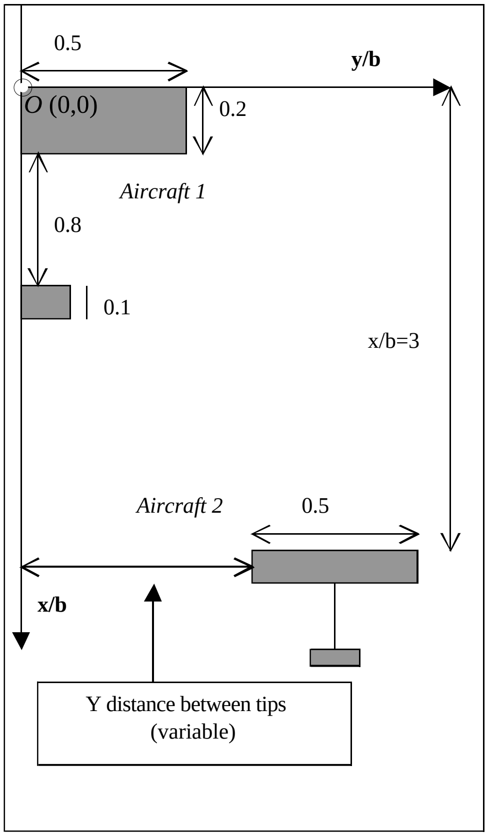

Figure 7. Geometry and relative movements between airplanes for different aircraft size configuration.

Table 2. Basic wing geometry for mother aircraft

Span	**1.0**
Geometric mean chord	**0.2**
Area	**0.2**
Aspect ratio	**5.0**
Taper ratio	**1.0**
Sweepback (quarter-chord line)	**0 deg**
Dihedral	**0**

The induced drag for *Aircraft 2* and the formation is again highly dependent of the relative spanwise distance between airplanes. *Aircraft 1* has a constant induced drag coefficient when airplane tips are not very close to each other. When *y/b* approaches 1, *Aircraft 1* experiences a sharp increase in induced drag that benefits the whole system of airplanes since the drag of *Aircraft 2* is highly decreased. Negative induced drag values (a thrust) are experienced by the trailing aircraft for *y/b* values lower that 1.05.

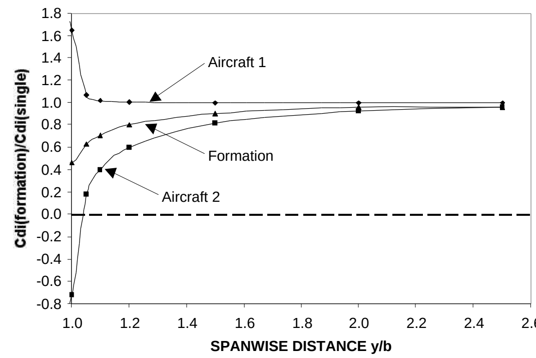

Figure 8. Spanwise effect for different aircraft size configuration, *x/b*=3.0, *z/b*=0.01

Elliptic load distributions, close to the optimum ones, are obtained for values of *y/b* greater than 1.05. It is in this region where the induced drag coefficient of *Aircraft 1* remains constant. When the tips come closer, the load distributions deviate from the elliptic shape and higher loads are found near the tips.

For this case, higher loads on the tips of the mother aircraft are even more beneficial, since they will cause a high upwash field that can be used by the smaller airplanes. The result is that optimum spanloads for close aircraft positions deviate more from the elliptical loading for this type of configuration.

Figure 9 shows the optimum load distributions for two cases. For *y/b*=1.0 the spanloads are very different from flying-alone optimums, resulting in an 80% increase in the induced drag of the mother aircraft and a negative induced drag on the smaller ones (see **Figure 8**). For *y/b*=1.05 the optimum spanloads are now nearly elliptic. *Aircraft 1* still has high loads near the tips because of the relative proximity between airplanes. *Aircraft 1* experiences an increase in induced drag of less than 10% while the trailing aircraft achieve drag reductions greater than 80%.

Again, overlapping tips means close vortex interactions, where the potential-flow vortex model may not be accurate.

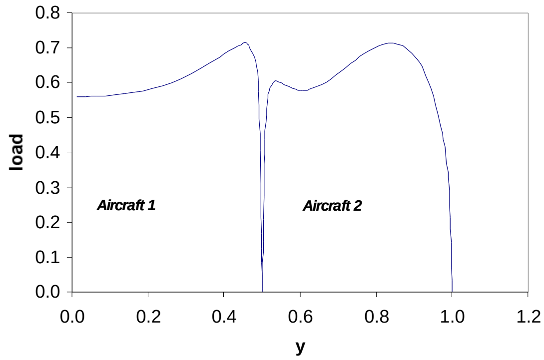

a) z/b = 0.01, y/b = 1.00

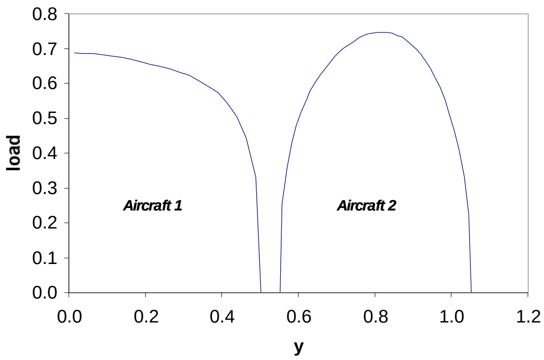

b) z/b = 0.01, y/b = 1.05

Figure 9. Optimum load distributions for different spanwise distances. Different aircraft size configuration.

VI. Optimum aircraft position

It seems that the ideal V-shape configuration will be that in which the induced drag of every airplane will be the same, so that each one of them obtains equal benefits. **Figure 2** shows that such a configuration requires close spacing between aircraft (*x/b*=0.1). A more realistic configuration will be that in which aircraft collision can be avoided. When *x/b* is high both in the negative and positive directions, the danger of collision is eliminated.

Besides collision avoidance, desired aircraft position is also limited by the ability of each airplane to maintain its position and optimum load distribution in the configuration.

It was noted above (see **Figures 5** and **9**) that the optimum load distribution is highly dependent on aircraft's relative position when airplanes overlap in the spanwise direction and they have a close vertical spacing. The key problem here is how to obtain different load distributions for different aircraft positions.

The approaches of Feifel[2] and Maskew[3] do not encounter that problem since their effective angle of attack at each station is known. Their only problem is finding the aileron deflection required to obtain a zero rolling moment about the center of gravity.

In this paper the entire wing is treated as a rolling-control surface. Moreover downwash velocities and optimum spanloads are dependent on aircraft position. A new twist distribution is needed (recall that planform geometry is always constant) for every configuration to achieve these load distributions.

Another problem exists for formation flying. For these cases the rapidly changing conditions when airplane tips are close to each other leads to highly varying rolling moment coefficients that require continuous aileron adjustments. Wolf, Chichka and Speyer[16] developed decentralized controllers and peak-seeking control methods to make these adjustments and maintain the aircraft at their optimum positions. For the peak-seeking control methods, due to the difficulties of measuring drag (or thrust) during flight, airplanes are maintained at a position where the rolling moment coefficient is a maximum. It is assumed that the maximum rolling moment coefficient occurs at the minimum induced drag location. This assumption may not always be true, so that real optimum positions are not necessarily obtained.

Beukenberg and Hummel[5] showed that with the application of such a maximum rolling moment control method in test flights, only half of the expected benefits could be achieved. Other control methods designed to maintain aircraft in formation have been developed,[7,18] but these methods do not include the strong aerodynamic effects that cause high rolling moments. Further work is required in this field before conclusions can be made.

For this case study, the changing spanload distributions in the overlap region will be difficult to obtain. However, important drag reductions can be obtained for a *y/b* greater than one (see **Figures 4** and **8**). In this region, the optimum load distribution is in fact nearly elliptic, very close to the solo flying optimum.

If the overlapping region is not a feasible solution for a formation configuration due to geometry or control problems, the induced drag benefits will be decreased. In the spanwise study for three equal aircraft, for example, induced drag reductions for *Aircraft 2* will go from 80% to around 40%, and total formation drag savings will decrease from 50% to about 30% (see **Figure 4**).

VII. Conclusions

A method has been developed to calculate the optimum load distribution for a group of aircraft flying in V-formation that gives minimum induced drag for the whole configuration. The method allows the study of induced drag coefficients for separate aircraft and the formation as a function of relative distance between airplanes. Only planform geometry is fixed for each aircraft in the formation, with no twist or camber distribution specified.

When the distance between airplanes is changed, the optimum load distribution giving minimum induced drag also changes. Twist distribution must then be changed as a function of aircraft distance if maximum induced drag savings are expected.

A test case has been studied consisting of three aircraft flying in an arrow formation. It has been shown that the optimum load distribution (and hence the optimum twist distribution) is highly dependent on spanwise distance when the aircraft tips are very close to each other or they overlap in this direction. When aircraft tips do not overlap in the spanwise direction the load distribution nearly approaches the optimum spanload when flying alone.

To avoid collisions between aircraft, they should be separated in the streamwise direction. Results show that for a large enough streamwise distance between aircraft (about three spans), induced drag coefficients for each airplane are no longer dependent on this direction. Induced velocities also become independent of the streamwise direction for these distances. A given twist distribution will provide then the desired optimum lift distribution in this region.

As long as the airplanes are in a not very sensitive region with respect to required twist distributions the induced drag reductions can be certainly obtained. For a configuration of three equal aircraft, with the central aircraft leading the formation and the other ones in a non-sensitive region, induced drag reductions for the formation of about 30% are achievable.

A formation with a mother aircraft leading two smaller airplanes half its size in a non-sensitive region can give formation drag reductions of 40%, with induced drag savings in the trailing aircraft greater than 80%.

Unfortunately, highly sensitive regions to required twist distribution coincide with regions of maximum drag savings. If aircraft were positioned in the aerodynamic optimum, with no regards to required geometries, induced drag reductions of 50% are possible for the equal aircraft formation. For the mother aircraft and its trailing partners, about 60% savings for the formation induced drag can be obtained, and the trailing aircraft would experience a negative induced drag (a thrust forward).

The results obtained here need to be extended to include the design wing shape. With the aircraft position and spanload known, the camber surface required to achieve the design spanload must be found.

References

[1]Shollenberger, C. A., and Lissaman, P., "Formation Flight of Birds," *Science*, May 1970.

[2]Feifel, W. M., "Optimization and Design of Three-Dimensional Aerodynamic Configurations of Arbitrary Shape by a Vortex Lattice Method," NASA SP-405, May 1976

[3]Maskew, B., "Formation Flying Benefits Based On Vortex Lattice Calculations," NASA CR-151974, April 1977.

[4]Jenkinson, L.R., Caves, R.E., and Rhodes, D.P., "Automatic Formation Flight," AIAA Paper 95-3898, Sept., 1995.

[5]Beukenberg, M., and Hummel, D., "Aerodynamics, performance and control of airplanes in formation flight," Technische Universität Braunschweig, Brunswick, Federal Republic of Germany. ICAS-90-5.9.3, Congress, 17th, Stockholm, Sweden, Sept.9-14, 1990.

[6]Blake, W., and Multhopp, D., "Design, Performance and Modeling Considerations for Close Formation Flight," AIAA Paper 98-4343, Aug., 1998.

[7]Gingras, D. R., "Experimental Investigation of a Multi-Aircraft Formation," AIAA-99-3143, 1999.

[8]Grasmeyer, J., "A Discrete Vortex Method for Calculating the Minimum Induced Drag and Optimum Load Distribution for Aircraft Configurations with Noncoplanar Surfaces" VPI-AOE-242, January 1997.

[9]Blackwell, J., "Numerical Method to Calculate the Induced Drag or Optimal Span Loading for Arbitrary Non-planar Aircraft." NASA SP-405, May 1976.

[10]Lamar, J., "A Vortex Lattice Method for the Mean Camber Shapes of Trimmed Non-Coplanar Planforms with Minimum Vortex Drag," NASA TN-D-8090, June 1976.

[11]Kuhlman, J., and Ku, T., "Numerical Optimization Techniques for Bound Circulation Distribution for Minimum Induced Drag of Nonplanar Wings: Computer Program Documentation." NASA CR-3458, 1982.

[12]Kroo, I., "A General Approach to Multiple Lifting Surface Design and Analysis", AIAA-84-2507, 1984.

[13]Munk, Max M., "The Minimum Induced Drag of Aerofoils," NACA Report No. 121, 1921.

[14]Tulinius, J., Clever, W., Nieman, A., Dunn, K., and Gaither, B., "Theoretical Prediction of Airplane Stability Derivatives at Subcritical Speeds", NASA CR-132681, Jan 1973.

[15]Iglesias, Sergio, "Optimum Spanloads Incorporating Wing Structural Considerations and Formation Flying." MS Thesis, Virginia Tech, November 2000 (available electronically from W.H. Mason's web site:
http://www.aoe.vt.edu/aoe/faculty/masfac.html

[16]Wolfe, J. D., Chichka, D. F., Speyer, J. L., "Decentralized Controllers for Unmanned Aerial Vehicle Formation Flight," AIAA-96-3833, 1996.

[17]McCamish, S., Pachter, M., D'Azzo, J. J., "Optimal Formation Flight Control," AIAA-96-3868, 1996.

[18]Dargan, J. L., Pachter, M., D'Azzo, J. J., "Automatic Formation Flight Control," AIAA-92-4473, 1992.